A statistical analysis of the correlation between large igneous provinces and lower mantle seismic structure

Geophysical Journal International

Geophys. J. Int. (2014) doi: 10.1093/gji/ggt500

Geophysical Journal International Advance Access published January 22, 2014

A statistical analysis of the correlation between large igneous provinces and lower mantle seismic structure

Jacqueline Austermann,[1] Bryan T. Kaye,[2] Jerry X. Mitrovica[1] and Peter Huybers[1]

[1] *Department of Earth and Planetary Sciences, Harvard University,* 20 *Oxford Street, Cambridge, MA* 02138*, USA. E-mail: jaustermann@fas.harvard.edu*
[2] *School of Engineering and Applied Sciences, Harvard University, 29 Oxford Street, Cambridge, MA* 02138*, USA.*

Accepted 2013 December 10. Received 2013 December 6; in original form 2013 July 10

SUMMARY

Large igneous provinces (LIPs) lie approximately above the margins of the African and Pacific large low shear velocity provinces (LLSVPs) in the deep mantle. This spatial correlation has been used to argue that plumes are preferentially generated at the margins of LLSVPs. We perform a series of Monte Carlo–based statistical tests to assess the uniqueness of this conclusion. These tests indicate that (1) the reconstructed locations of LIPs are significantly correlated with both slower-than-average shear wave velocity regions, which contain LLSVPs, and the margins of these structures; and (2) these correlations cannot be statistically distinguished. That is, given current constraints, if plumes were generated randomly throughout regions of slower-than-average shear wave velocity in the deep mantle, then statistical tests are expected to show a significant correlation between the locations of LIPs and the margins of LLSVPs. We therefore conclude that it is premature to argue that the margins of LLSVPs represent preferred zones of plume generation. This conclusion is reinforced in our analysis by a demonstration that the expected mean distance of a set of points randomly placed in slower-than-average shear wave velocity regions is consistent with the observed mean distance between LIPs and the margins of LLSVPs. Finally, we also test the correlation between the reconstructed locations of LIPs and the horizontal gradient in deep mantle shear velocity perturbations. We find, given the uncertainty implied by different tomography models, that there is no statistically significant correlation and that being in a slow region (i.e. in the region of LLSVPs) is a stronger geographic requirement for plume generation than being at a specific (high) gradient.

Key words: Spatial analysis; Seismic tomography; Dynamics: convection currents, and mantle plumes; Large igneous provinces.

1 INTRODUCTION

Large igneous provinces (LIPs) are regions where basaltic lava formed during massive eruptions of relatively short duration (Coffin & Eldholm 1994). They have ages ranging from 15 to 300 Ma (Torsvik *et al*. 2006; Torsvik *et al*. 2008a) and are commonly associated with plumes originating from the core-mantle boundary (CMB) (e.g. Richards *et al*. 1989), although a shallow origin has also been postulated (Anderson 1982). It has been recognized that LIPs correlate spatially with low shear wave velocity structures in the lower mantle (e.g. Burke & Torsvik 2004). However, efforts to establish this correlation face several complications. First, one has to restore the LIPs to their location on the Earth's surface at the time of their formation using models of plate motions. Second, one has to restore present-day shear wave velocity anomalies in the lower mantle to the time of putative plume generation, which is presumably older than the time of LIP eruption. In practice, this latter restoration has been avoided by assuming that seismic velocity anomalies are stable (i.e. stationary) in the highly viscous deep mantle.

At their restored locations, LIPs appear to be close to the (surface projected) edges of the two large low shear velocity provinces (LLSVPs) at 2800 km depth (Fig. 1a). On this basis, Torsvik *et al*. (2006) chose a specific shear wave velocity anomaly contour (e.g. −1 per cent for SMEAN; Becker & Boschi 2002) to describe margins of LLSVPs and postulated that deep mantle plumes are generated close to this contour. Burke *et al*. (2008) presented additional comparisons with D″ models and a statistical analysis to support their argument of a spatial correlation between restored LIP locations and margins of LLSVPs and smaller low shear velocity provinces (LSVPs). They subsequently referred to those margins as the plume generation zone. Torsvik *et al*. (2006) have, furthermore, argued that LIPs correlate with regions of steep gradients in deep mantle velocity perturbations (Fig. 1b).

The conclusion that LIPs are preferentially generated at margins of LLSVPs has been cited in studies that tried to constrain longitude in palaeomagnetic reconstructions (Torsvik *et al*. 2008b), proposed locations for kimberlite and diamond exploration (Evans 2010; Torsvik *et al*. 2010), and explored the implications for mantle convection (e.g. Steinberger & Torsvik 2012). Moreover,

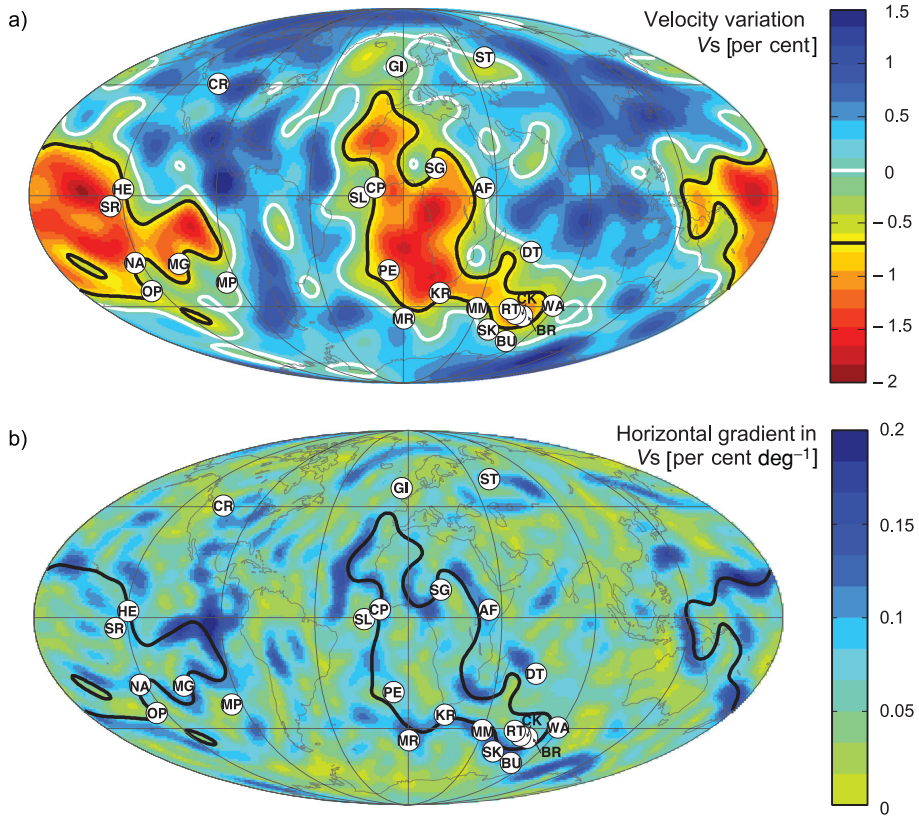

Figure 1. LIP locations (white circles) restored to their original position using a global palaeomagnetic reference frame. The abbreviation for each LIP is taken from table 1 of Torsvik *et al*. (2006). (a) The colour scale shows the per cent perturbation in shear wave velocity relative to a 1-D model (*Vs*) at 2800 km depth from the seismic tomography model S20RTS. These are perturbations relative to the Preliminary Reference Earth Model (PREM; Dziewonski & Anderson 1981). The thick black line highlights the −0.65 per cent value used by Torsvik *et al*. (2006) to define the margin of LLSVPs, and the white line shows the 0 per cent contour. Analogous figures based on other seismic tomography models are provided in Torsvik *et al*. (2006) and Burke *et al*. (2008). (b) The colour scale shows the smoothed magnitude of the horizontal gradient in shear wave velocity anomalies at 2800 km depth calculated using the S20RTS seismic tomography model. The reconstructed LIP locations and thick black line are reproduced from frame (a).

since there is evidence for LIPs as old as 2.5 Gy (Ernst & Buchan 2003), Burke *et al*. (2008) have argued that LLSVPs have been relatively stable over such long timescales, which makes them candidates for geochemical reservoirs of primordial mantle (e.g. Mukhopadhyay 2012).

The net buoyancy of LLSVPs is a matter of contention. Published studies have argued that thermal effects on density dominate chemical effects and that LLSVPs are positively buoyant (Forte & Mitrovica 2001; Davies *et al*. 2012; Schuberth *et al*. 2012) or that the reverse is true and LLVSPs are negatively buoyant thermochemical piles (McNamara & Zhong 2005; Bull *et al*. 2009). However, regardless of the net buoyancy of LLSVPs, the consensus that they represent hotter than average mantle structures suggests that the entire surface of LLSVPs may act as zones of plume generation. This suggestion is supported by the recent seismic imaging of a plume originating from top surface of the LLSVP below Africa (Sun *et al*. 2010).

In this study, we present a new statistical analysis of the spatial correlation between LIPs and (1) the margins of LLSVPs, (2) the full areal extent of LLSVPs and (3) deep mantle regions characterized by the highest seismic velocity gradients. In the discussion below, we will include LSVPs in the term LLSVPs. Furthermore, unless otherwise stated, whenever we refer to LIP locations we mean the restored location of the initial eruption site.

2 LIPS, TOMOGRAPHY MODELS AND REFERENCE FRAMES

Following the analysis of Torsvik *et al*. (2006), we adopt three seismic tomographic inferences of mantle shear wave velocity heterogeneity: NGRAND (Grand 2002), S20RTS (Ritsema & van Heijst 2000) and SB4L18 (Masters *et al*. 2000). We also consider the D″ tomography model of Kuo *et al*. (2000) that was used by Burke *et al*. (2008). In contrast to this previous work, we do not use SMEAN (Becker & Boschi 2002), which combines the shear wave velocity models NGRAND, S20RTS and SB4L18, but instead base our statistical analysis on the three individual tomography models. This procedure provides a measure of the uncertainty related to errors in the tomography models.

Torsvik *et al*. (2006) reconstructed the position of LIPs at their time of formation using four different reference frames: global palaeomagnetic, Africa fixed hotspot, Africa moving hotspot and global moving hotspot. We do the same. Moreover, following Burke *et al*. (2008), we added the Skagerrak-Centred LIP (SK) proposed by Torsvik *et al*. (2008a) to the list of LIPs with a reconstructed location using the global palaeomagnetic reference frame.

Fig. 1(a) shows the reconstructed locations of LIPs using a global palaeomagnetic reference frame superimposed on the shear wave velocity map at the 2800 km depth slice of S20RTS. Names, symbols, ages and locations of LIPs can be found in table 1 of

Torsvik *et al*. (2006). The figure also shows the −0.65 per cent contour of velocity perturbation (*Vs*) in black, which Torsvik *et al*. (2006) define as the margin of the LLSVPs in the S20RTS tomography model. Following their argument, the margin-defining contours for the NGRAND, SB4L18 and Kuo *et al*. (2000) models are −1, −0.6 and −0.77 per cent, respectively (Torsvik *et al*. 2006; Burke *et al*. 2008). We adopt these choices in our statistical analyses.

For the analysis of the horizontal gradient of seismic velocity, we apply a 5° × 5° smoothing to the raw gradients. This processing makes steep gradients visually more evident. Fig. 1(b) shows the (smoothed) horizontal gradients in seismic velocity model S20RTS at 2800 km depth. The reconstructed LIP positions and the −0.65 per cent contour of the velocity perturbation are reproduced from Fig. 1(a).

3 CORRELATION BETWEEN LIPS AND LOWER MANTLE SEISMIC STRUCTURE

The statistical analysis of Burke *et al*. (2008) was based on the following question: If LIPs are the result of plumes generated at random locations in the deep mantle, how likely is the observed proximity of the LIPs to the margins of LLSVPs? To answer this question, they first determined the number of LIPs that are located within a specific angular distance from the margin of LLSVPs: Using the tomography by Kuo *et al*. (2000) and the palaeomagnetic reference frame for LIP reconstructions, 16 of 24 LIPs have an angular distance of 5° or less from the margins of LLSVPs. They next determined the probability that 16 or more randomly chosen points on the Earth's surface were located within this distance of the margins of LLSVPs, which they found to be very low (less than 0.1 per cent). Similar results were obtained for analyses based on the other tomographic models of shear wave heterogeneity. On this basis, they concluded that LIPs are not located randomly on the Earth's surface, and that the margins of LLSVPs serve as zones of plume generation.

Since LLSVPs are hotter than the surrounding mantle, their entire surface may act as zones of plume generation. This raises the question: Are the observed locations of LIPs statistically correlated with slower-than-average shear wave velocity regions (i.e. LLSVPs) and, if so, is the previously identified correlation between LIP locations and the margins of LLSVPs statistically distinguishable from this new test of correlation? If the answer to the former question is yes and the latter is no, then the correlation of LIP locations with LLSVP margins may simply be part of a more general correlation between these locations with LLSVPs themselves. In this case, it would be premature to conclude that the margins of LLSVPs act as a plume generation zone.

To address these issues, we first conducted a series of Monte Carlo–based statistical tests that follow the approach of Burke *et al*. (2008). Specifically, we ran 1000 simulations in which we randomly positioned 24 points on a sphere. These points were drawn from a distribution that is uniform in space. In each case, we calculated: (1) the mean angular distance of the points from the (surface projected) LLSVP margins; and (2) the percentage of points that overlie slower-than-average shear wave velocity anomalies at the 2800 km depth slice of a tomographic model. We consider observed LIPs to be spatially correlated with margins of LLSVPs if their mean angular distance from these margins is smaller than 95 per cent of the mean angular distances obtained in the Monte Carlo sampling. Similarly, we consider observed LIPs to be spatially correlated with slower-than-average shear wave velocities if the percentage of LIPs that overlie slower-than-average shear wave velocity anomalies is greater than 95 per cent of the percentages obtained in the Monte Carlo sampling. That means all tests will be performed at the 95 per cent significance level and we assume that LIPs are independent of one another, that is, there is no clustering beyond just being near LLSVPs.

Figs 2(a) and (b) show the observed values (red lines) and the distribution that we obtain from the Monte Carlo sampling (blue histograms) when the above tests are applied to the S20RTS tomography model and the LIP reconstruction based on the palaeomagnetic reference frame. The observed mean angular distance between the LIPs and the LLSVP margins is 8° (Fig. 2a) and the percentage of LIPs that overlie slower-than-average regions is 87.5 per cent (21 of 24). The former is smaller than all of the mean angular distances obtained from the 1000 Monte Carlo samples, and we therefore conclude that the observed locations of LIPs are correlated with margins of LLSVPs. The latter percentage is greater than all of the percentages obtained from Monte Carlo sampling and we therefore conclude that the observed locations of LIPs are also correlated with slower-than-average shear wave velocities (i.e. LLSVPs). We have repeated the above tests for all possible combinations of tomography models and reference frames for LIP reconstruction and the same conclusions hold in each case.

The next Monte Carlo test is designed to address the following question: If LIPs are the result of plumes generated throughout regions of slower-than-average seismic velocity (LLSVPs), does this naturally lead to a correlation between the observed location of LIPs and the margins of LLSVPs? In this test, we ran 1000 simulations in which we randomly positioned 24 points within (surface projected) zones of slower-than-average seismic velocity. In each case, we calculated the mean angular distance of these points from the margins of LLSVPs. A histogram of the results is shown (in red) in Fig. 2(c). This histogram indicates that in 99.9 per cent of all samples, the mean angular distance to the margin of LLSVPs is smaller than 95 per cent (significance level) of the mean angular distances obtained in the first test (i.e. the histogram in Fig. 2c falls entirely within the blue shaded region defined by the histogram in Fig. 2a). That is, in almost all cases when plumes are generated in regions of slower-than-average shear wave velocity, they are also closer to the margins of LLSVPs than if they were randomly distributed around the globe. We conclude that a seemingly significant relationship between the location of LIPs and margins of LLSVPs will generally arise if plumes are generated in slower-than-average shear wave velocity regions and evaluated against a null hypothesis of a globally uniform distribution. Further testing indicates that this conclusion holds regardless of the combinations of seismic tomography models and reference frames for LIP reconstruction. As a final point, it is interesting to note that the peak in the histogram in Fig. 2(c), that is, the most likely mean angular distance to the margin of LLSVPs when plumes are randomly generated from LLSVPs, matches the observed mean angular distance of LIPs from the margins of LLSVPs.

In the next Monte Carlo test, we address the following variation on the last question: If LIPs are the result of plumes generated at the margins of LLSVPs, does this naturally lead to a correlation between the observed location of LIPs and regions of slower-than-average seismic velocity (LLSVPs)? In this case, we ran 1000 simulations in which 24 points were randomly positioned within a zone close to margins of LLSVPs, where 'close' means that the distance follows a half-normal distribution with standard deviation of 5°. In each case, we computed the percentage of points that overlie zones of slower-than-average seismic velocity; a histogram of the results is

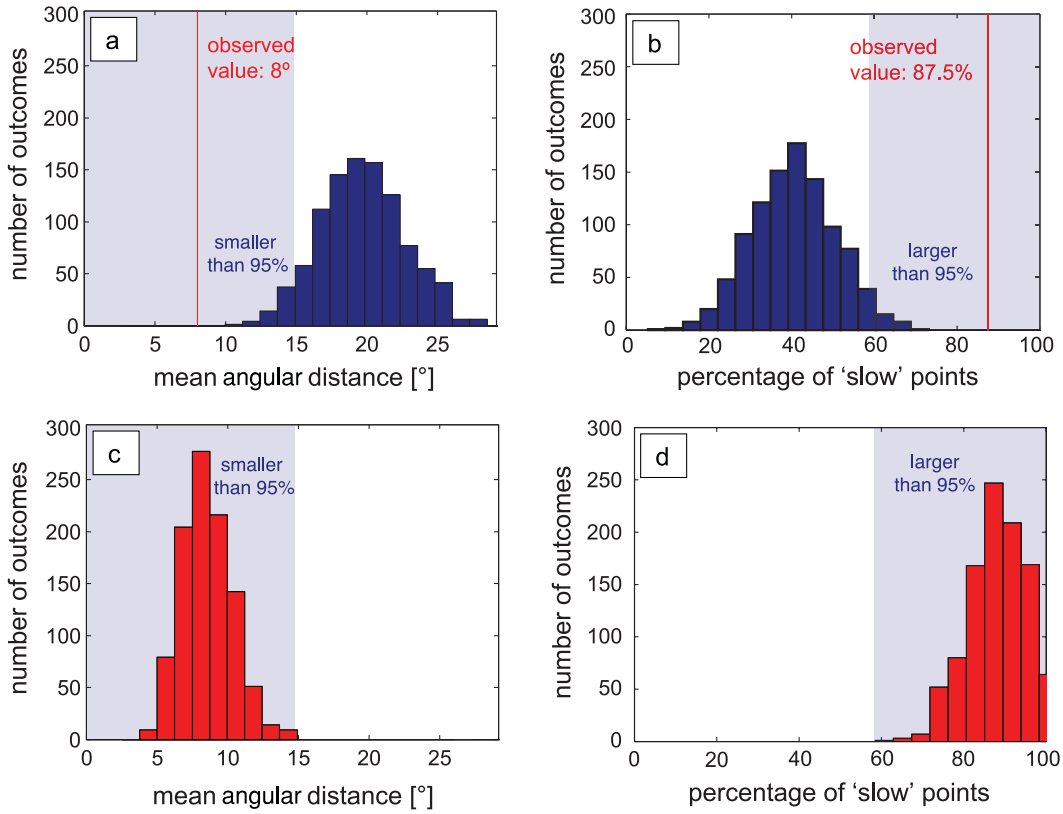

Figure 2. Results of Monte Carlo statistical testing (1000 samples) based on the S20RTS seismic tomography model at 2800 km depth and the palaeomagnetic reference frame for LIP reconstruction. (a) The distribution of mean angular distances to the margins of LLSVPs (horizontal axis) when 24 points are randomly positioned on the globe. The red vertical line denotes the value obtained from the reconstructed LIP locations. The light blue region indicates the range of mean angular distances that are smaller than 95 per cent of the mean angular distances obtained from Monte Carlo sampling. (b) Same as frame (a), except for the distribution of the percentage of points that overlie regions of slower-than-average ('slow') seismic shear wave velocity at 2800 km depth in the mantle. In this case, the light blue indicates the range of percentages that are larger than 95 per cent of the percentages obtained from Monte Carlo samples. (c) The distribution of mean angular distances to the margins of LLSVPs when 24 points are randomly positioned in regions of slower-than-average seismic shear wave velocity at 2800 km depth. The blue shaded region is the same as in frame (a). (d) The distribution of the percentage of points located in regions of slower-than-average seismic velocity at 2800 km depth when they are randomly positioned close to margins of LLSVPs (where 'close' is defined quantitatively in the text). The blue shaded region is the same as in frame (b).

shown (in red) in Fig. 2(d). This histogram indicates that, in every one of the 1000 Monte Carlo samples, the percentage of points that overlie zones of slower-than-average seismic velocities is greater than 95 per cent (significance level) of the percentages obtained in the Monte Carlo analysis summarized in Fig. 2(b). This result is in line with the geometric rational that the slower-than-average contour resides, on average, 7.7° outside of the contour that denotes the margin on LLSVPs and serves to highlight that distinguishing between a contour of high gradient and region of slow velocity is, in this case, geometrically and statistically difficult. We conclude that a statistically significant correlation between the location of LIPs and regions of slower-than-average seismic velocity (LLSVPs) is the expected consequence of plumes being generated near the margins of LLSVPs. We repeated the analysis of Fig. 2(d) for all possible combinations of tomography models and reference frames for LIP reconstruction. In all cases, at least 90 per cent of the realizations analogous to those shown in Fig. 2(d) were greater than 95 per cent (significance level) of the realizations shown in Fig. 2(b). This means that the above conclusion (that points which lie close to margins of LLSVPs also tend to lie over slower-than-average seismic velocity perturbations) is independent of the adopted tomography model. Note that the peak in the histogram in Fig. 2(d), that is the most likely percentage of points within slow regions when plumes are randomly generated at the margins of LLSVPs, matches the observed percentage of LIPs that lie above slower than average mantle at 2800 km depth.

The results discussed above may be sensitive to several assumptions that were made in the analyses. First, consider our adoption of a 95 per cent significance level. If we had chosen a more stringent significance level of 99 per cent, then the shaded blue regions in all of the frames in Fig. 2 would decrease. Our conclusions based on a comparison of the observed values with the histograms in Figs 2(a) and (b) would not have been altered in this case, but the conclusions from our test comparing the histograms in Figs 2(c) and (d) with the histograms in Figs 2(a) and (b), respectively, would have been marginally weakened. That means, the percentage of realizations that falls within the significance level of 99 per cent drops to 99.1 per cent for the test shown in Fig. 2(c), but stays at 100 per cent for the test shown in Fig. 2(d). Second, in regard to Fig. 2(d), one might question our adoption of a half-normal distribution with a standard deviation of 5° to define 'closeness'. Increasing this standard deviation would move the (red) histogram in Fig. 2(d) to lower values. As an example, increasing the standard deviation to 10° (which would produce a mean angular distance of 8°) moves the peak of

the histogram to ∼70 per cent. Third, in regard to Fig. 2(c), one might argue that not all LIPs lie over slower-than-average regions, so we should only locate some arbitrarily large fraction of the 24 points in slower-than-average regions and the rest in colder-than-average regions. Using a fraction less than the 100 per cent adopted in the test summarized in Fig. 2(c) would move the histogram to higher mean angular distances. As an example, repeating the test in Fig. 2(c) for a case in which 87.5 per cent of the points are located within regions of slower-than-average seismic velocity moves the peak of the histogram to ∼10°.

In defence of the choices we made concerning the second and third assumptions listed above, we note again that the histograms in Figs 2(c) and (d) are approximately centred on the observed values (red lines in Figs 2a and b). This suggests that our choices led to a reasonable distribution of results in the Monte Carlo tests.

4 CORRELATION BETWEEN LIPS AND HIGH SEISMIC VELOCITY GRADIENTS IN THE DEEP MANTLE

Previous studies have argued for a correlation between regions of high horizontal gradient in seismic shear wave velocity in the deep mantle and various surface expressions of plumes. For example, Thorne *et al*. (2004) found that such regions are correlated to present-day hotspot locations. However, independent analyses (Courtillot *et al*. 2003; Montelli *et al*. 2006; Torsvik *et al*. 2006) suggest that only 11 of the 44 hotspots that were used in the Thorne *et al*. (2004) analysis can be identified as having a deep origin. As we noted in the introduction, Torsvik *et al*. (2006) argued that the margin of LLSVPs (the region they defined as the plume generation zone) was correlated with zones of high seismic velocity gradients. Indeed, a zone defined by some specific range in velocity gradients in the deep mantle might be a better candidate for a plume generation zone than a specific seismic velocity contour because instabilities in the boundary layer, which are thought to initiate plumes, are driven by gradients in temperature rather than absolute temperature. Fig. 1(b), which juxtaposes these zones with the locations of LIPs, suggests that it would be worthwhile to rigorously test the robustness of the correlation between these two.

Consider, once again, the Monte Carlo simulation based on repeatedly locating a set of 24 points randomly on the Earth's surface (as in the results summarized in Figs 2a and b). For each of the 1000 samples, we compute the mean value of the (magnitude of) horizontal gradients in the seismic velocity that underlie these 24 points. We consider LIPs to be spatially correlated with high horizontal gradients in seismic velocity if the mean gradient in velocity perturbations that LIPs overlie is greater than 95 per cent of the mean gradients determined in the Monte Carlo procedure.

Fig. 3 summarizes the results of our test for all combinations of seismic tomography model and reference frames for LIP reconstruction. For each of these combinations, the *y*-axis represents the percentage of the set of 1000 mean gradients that is exceeded by the mean gradient that the LIPs overlie. The results in Fig. 3 vary across a wide range. Except for the model using the African moving reference frame, all combinations that adopt the NGRAND seismic tomography model show that a statistically significant percentage of LIPs are in proximity to high seismic velocity gradients. In contrast, none of the tests based on combinations adopting either the SB4L18 or Kuo *et al*. (2000) tomography models show a statistically significant (to a 95 per cent level) correlation. Finally, of the tests based on the S20RTS tomography model, the LIP reconstructions based

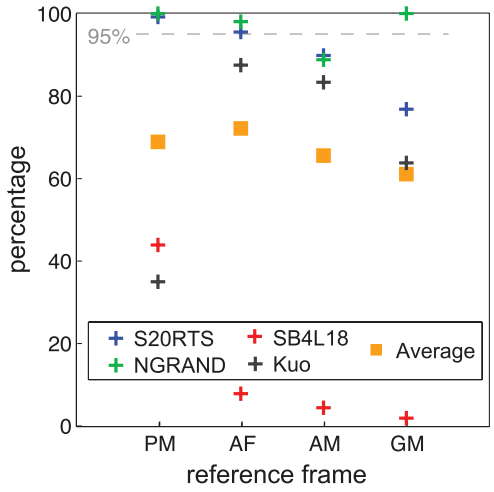

Figure 3. Results of Monte Carlo testing of the correlation between the location of LIPs and regions of high horizontal gradient in seismic velocity perturbations at 2800 km depth. 1000 sets of 24 points were randomly placed on the Earth's surface and the mean gradient in deep mantle seismic velocity that these points overlie is computed in each case. The ordinate axis represents the percentage of this set of 1000 mean gradients that is exceeded by the observed mean gradient that the LIPs overlie. The symbols represent results of the Monte Carlo tests based on different seismic velocity models (as labelled in the inset) and, in each case, the abscissa bins results according to the reference frame adopted in the reconstruction of LIP locations (PM, palaeomagnetic; AF, Africa fixed; AM, Africa moving; GM, global moving). Orange squares denote average values obtained for each reference frame.

on the palaeomagnetic and the African fixed reference frame lead to a significant correlation. The average value of the suite of results in Fig. 3 is ∼70 per cent. (This average is 85 per cent if the SB4L18 tomography model is not considered, although we have no *a priori* reason to discount this model.) We thus conclude that the proximity of LIPs to high seismic shear wave velocity gradients in the deep mantle is not necessarily statistically significant, given current uncertainties in deep mantle seismic tomography and the appropriate choice of reference frames, nor is it necessarily diagnostic of a physical relationship because proximity to high gradients is readily conflated with proximity to LLSVPs.

Despite this conclusion, it will be instructive to repeat the analysis in Fig. 2 replacing the distance-to-margin metric with a metric based on the magnitude of the velocity gradient. As in Fig. 2, we will adopt, for the purpose of illustration, the S20RTS tomography model and the palaeomagnetic reference frame. From Fig. 3, the mean horizontal gradient in seismic velocity underlying the 24 LIPs in this case is greater than 95 per cent of the mean gradients of the 1000 simulations in which the 24 points were randomly located on the Earth's surface (see Fig. 4a). In the case of a Monte Carlo simulation in which the 24 random points were restricted to lie above slower than average mantle at 2800 km depth (Fig. 4c), the mean seismic velocity gradients of ∼ 40 per cent of the simulations exceed 95 per cent of the gradients obtained in Fig. 4(a). The peak value of this distribution does not coincide with the observed value. To continue, Fig. 4(b), reproduced from Fig. 2(b), shows the percentage of points that overlie slower than average mantle at 2800 km depth when these points are placed randomly on the Earth's surface. In Fig. 4(d), we repeat the Monte Carlo test by placing the 24 points within regions of high gradient, that is, at gradients that exceed 0.04 per cent deg^{-1} (the observed values in gradients that LIPs overlie range from approximately 0.04 to 0.11 per cent deg^{-1}). We find that

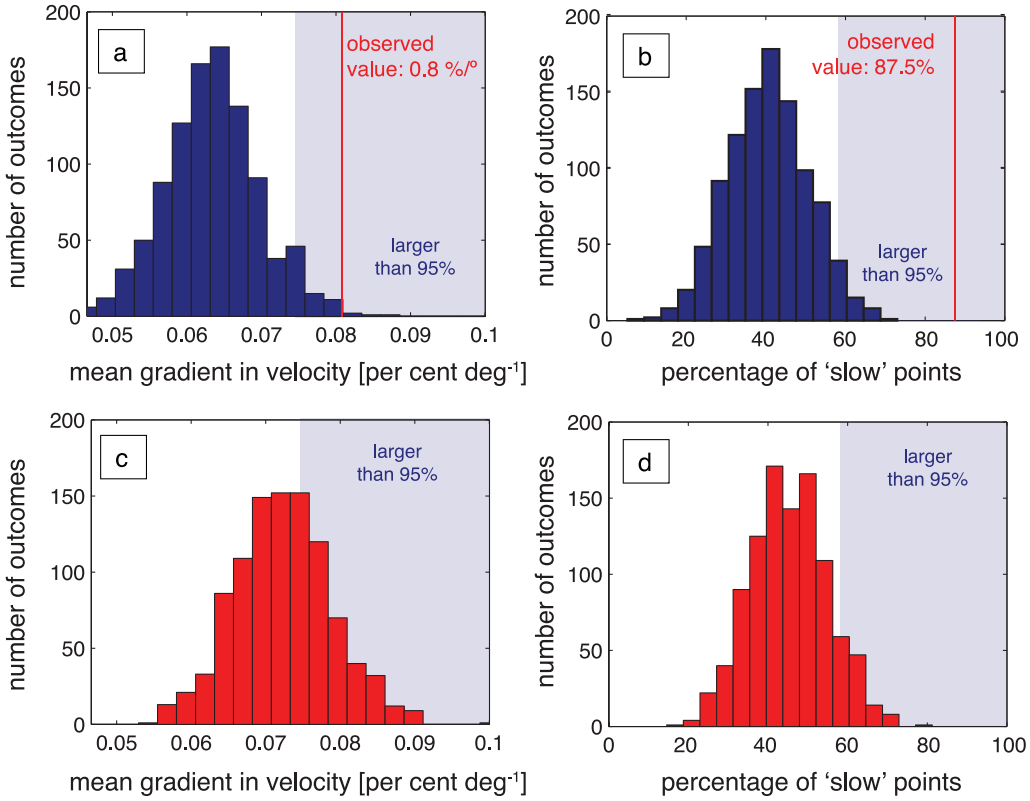

Figure 4. Results of Monte Carlo statistical testing (1000 samples) based on the S20RTS seismic tomography model at 2800 km depth and the palaeomagnetic reference frame for LIP reconstruction. (a) Distribution of the mean seismic velocity gradient (horizontal axis) for 24 points that are randomly positioned on the globe. The red vertical line denotes the value obtained from the reconstructed LIP locations. The light blue region indicates the range of mean gradients that are greater than 95 per cent of the mean gradients obtained from Monte Carlo sampling. (b) Same as frame (a), except for the distribution of the percentage of points that overlie regions of slower-than-average ('slow') seismic shear wave velocity at 2800 km depth in the mantle. This frame is reproduced from Fig. 2(b). The light blue region indicates the range of percentages that are larger than 95 per cent of the percentages obtained from Monte Carlo samples. (c) The distribution of the mean seismic velocity gradient when 24 points are randomly positioned in regions of slower-than-average seismic shear wave velocity at 2800 km depth. The blue shaded region is the same as in frame (a). (d) The distribution of the percentage of points located in regions of slower-than-average seismic velocity at 2800 km depth when they are randomly positioned within regions of high seismic velocity gradient (defined by gradients that exceed 0.04 per cent deg^{-1}). The blue shaded region is the same as in frame (b).

the positioning of plumes in this manner does not necessarily lead to a high percentage of the plumes being located above slower than average mantle at 2800 km depth, as is the case for the observed location of LIPs (Fig. 4b). Indeed, only 13 per cent of the simulations in Fig. 4(d) have a percentage of points in slow regions that exceed 95 per cent of the simulations in Fig. 4(b). These results indicate that LLSVPs might be a better geographic description for the preferred location of plumes than high gradients in velocity.

We performed an additional Monte Carlo test to explore this further (see Appendix for details). We once again adopted the S20RTS tomography model and randomly placed plumes in slow and fast regions at 2800 km depth in a relative number that is consistent with the observed sampling of these regions by LIPs (i.e. 21 of 24 are placed in slow regions). We found that this procedure reproduces well the observed range in seismic velocity gradients sampled by LIPs. However, the inverse does not hold. In particular, we performed an additional Monte Carlo test in which plumes were randomly placed in a manner that matched the observed distribution of seismic velocity gradients sampled by LIPs. In this case, the plumes sampled seismic velocities that were significantly faster (with 95 per cent confidence) than the velocities sampled by LIPs. This confirms that being located above seismically slow deep mantle regions (i.e. in the region defined by LLSVPs) is a stronger geographic requirement for plume generation than being located in a specific range of high seismic velocity gradients at 2800 km depth.

It is important to note that this result does not imply that high temperature gradients are unimportant in plume generation. This is because first, gradients in shear velocity near the CMB may be strongly controlled by chemical heterogeneities and second, limiting the analysis to velocity gradients at sites at 2800 km depth ignores the 3-D geometry of the surface characterized by a high seismic velocity gradient.

5 DISCUSSION

We conclude, on the basis of current constraints on LIP locations, seismic shear wave velocity heterogeneities in the deep mantle and plate motions, that the reconstructed locations of LIPs are correlated with both LLSVPs and the margins of these structures. However, we also conclude, given these current constraints, that these two correlations cannot be statistically distinguished at a 95 per cent confidence level. Our conclusions indicate that it is therefore premature to argue, as in some previous studies (Torsvik *et al*. 2006; Burke *et al*. 2008), that the margins of LLSVPs represent plume generation zones.

This conclusion is strengthened by noting that there are other substantial uncertainties that have not been quantified in these statistical analyses, including the lateral deflection of plumes during their ascent, incomplete knowledge of LIP locations with respect to the corresponding plume impact site on the base of the lithosphere and the appropriate depth at which the geographic extent of LLSVPs are defined. Torsvik *et al*. (2006) estimate the combined uncertainty of the first two of these effects to be ∼ 500 km. However, Steinberger (2000) estimated that the plume conduit can be deflected by as much as 800 km in the trajectory of a plume rising from the D″ region to the asthenosphere. (This deflection may be smaller if plumes are anchored at high points along the interface between LLSVPs and the overlying mantle.) In addition, given the evident clustering, it is not clear whether each LIP observation provides an independent constraint. This issue has direct implications for the analysis since fewer effective independent observations lead to less statistically significant results.

Our analysis has not considered hotspot data, including for example the tabulation by Steinberger (2000). As discussed above, not all (Steinberger 2000; Courtillot *et al*. 2003; Torsvik *et al*. 2006), if any (Anderson 1982), of these hotspots can be sourced to the deep mantle. Moreover, some of these hotspots are thought to originate from the same plumes associated with LIPs, and they therefore do not provide an entirely independent data set.

The mechanisms for plume formation remain poorly constrained and controversial. The correlation we have identified between the location of LIPs and the areal extent of LLSVPs is consistent with the recent seismic imaging of a plume-like structure rising from the upper surface of the LLSVP beneath Africa (Sun *et al*. 2010), and, more generally, with the suggestion by Kellogg *et al*. (1999) that plumes would tend to arise from local high spots along the surface of LLSVPs.

In mantle convection models, the location of plume formation related to LLSVPs depends strongly on the buoyancy and geometry of these structures (e.g. Tan *et al*. 2011). Plumes are generally sourced from warm mantle material that rises along the slope of LLSVPs when the latter are modelled as having high density. In this case, if LLSVPs have steep slopes, plumes will tend to originate at their margins (when the LLSVPs are mapped in plan view), whereas shallow slopes lead to material rising from crests along the upper surface of LLSVPs. Furthermore, to be stable over long timescales, LLSVPs need to have a minimum integrated negative buoyancy. Tan *et al*. (2011) used convection models to explore LLSVP geometries and the location of plume generation. They found that when LLSVPs were assigned a high bulk modulus and high density in their models, they would form a dome-like geometry with plumes emerging from the steep margins. However, the lateral position of these structures was only stable for periods longer than a few hundred million years if the subduction geometry was relatively stationary in time. Steinberger & Torsvik (2012) proposed a strong coupling between deep mantle processes and plate tectonics to explain the formation of plumes along margins of LLSVPs. They introduced sinking slabs (constrained by plate reconstructions) that push heavy chemical material into piles with steep edges. Moreover, these slabs deform the thermal boundary layer at the CMB initiating upward motion of hot material along the steep edges of LLSVPs and plume generation.

Clearly, the argument that plume formation occurs at the margins of LLSVPs has been an important motivation for recent studies of mantle convection. The implication of our statistical analysis is that the conclusions from these studies regarding the thermochemical structure of the LLSVPs, and their long-term stability, may not be robust. An improved understanding of this thermochemical structure, and its relationship to plume generation, will come from advances in lower mantle composition and mineral physics (e.g. Mattern *et al*. 2005; Irifune *et al*. 2010), in combination with geodynamic modelling of global geophysical observables (Forte & Mitrovica 2001), seismic imaging of the steepness of LLSVPs (Ni *et al*. 2002; To *et al*. 2005; He & Wen 2009) and plume conduits (Montelli *et al*. 2006; Boschi *et al*. 2007), geochemistry of LIPs and ocean island basalts, (Chabaux & Allègre 1994; Bourdon *et al*. 2006; Sobolev *et al*. 2011) and the incorporation of plate motions into thermochemical convection models (McNamara & Zhong 2005; Zhang *et al*. 2010; Steinberger & Torsvik 2012; Bower *et al*. 2013).

ACKNOWLEDGEMENTS

We would like to thank Shijie Zhong and Christine Houser for their comments and Bernhard Steinberger for helpful suggestions. Support for this research was provided by Harvard University and the Canadian Institute for Advanced Research.

REFERENCES

Anderson, D.L., 1982. Hotspots, polar wander, Mesozoic convection and the geoid, *Nature,* **297,** 391–393.

Becker, T. & Boschi, L., 2002. A comparison of tomographic and geodynamic mantle models, *Geochem. Geophys. Geosyst.,* **3,** doi:10.1029/2001GC000168.

Bull, A.L., McNamara, A.K. & Ritsema, J., 2009. Synthetic tomography of plume clusters and thermochemical piles, *Earth planet. Sci. Lett.,* **278,** 152–162.

Burke, K. & Torsvik, T.H., 2004. Derivation of large igneous provinces of the past 200 million years from long-term heterogeneities in the deep mantle, *Earth planet. Sci. Lett.,* **227,** 531–538.

Burke, K., Steinberger, B., Torsvik, T.H. & Smethurst, M.A., 2008. Plume generation zones at the margins of large low shear velocity provinces on the core-mantle boundary, *Earth planet. Sci. Lett.,* **265,** 49–60.

Boschi, L., Becker, T.W. & Steinberger, B., 2007. Mantle plumes: dynamic models and seismic images, *Geochem. Geophys. Geosyst.,* **8**(10), Q10006, doi:10.1029/2007GC001733.

Bourdon, B., Ribe, N.M., Stracke, A., Saal, A.E. & Turner, S.P., 2006. Insights into the dynamics of mantle plumes from uranium-series geochemistry, *Nature,* **444,** 713–717.

Bower, D.J., Gurnis, M. & Seton, M., 2013. Lower mantle structure from paleogeographically constrained dynamic Earth models, *Geochem. Geophys. Geosyst.,* **14**(1), doi:10.1029/2012GC004267.

Chabaux, F. & Allègre, C.J., 1994. ^{238}U-^{230}Th-^{226}Ra disequilibria in volcanics: a new insight into melting conditions, *Earth planet. Sci. Lett.,* **126,** 61–74.

Coffin, M.F. & Eldholm, O., 1994. Large igneous provinces—crustal structure, dimension, and external consequences, *Rev. Geophys.,* **31**(1), 1–36.

Courtillot, V., Davaille, A., Besse, J. & Stock, J., 2003. Three distinct types of hotspots in the Earth's mantle, *Earth planet. Sci. Lett.,* **205,** 295–308.

Davies, D.R., Goes, S., Davies, J.H., Schuberth, B.S.A., Bunge, H.-P. & Ritsema, J., 2012. Reconciling dynamic and seismic models of Earth's lower mantle: the dominant role of thermal heterogeneity, *Earth planet. Sci. Lett.,* **353–354,** 253–269.

Dziewonski, A.M. & Anderson, D.L., 1981. Preliminary Reference Earth Model, *Phys. Earth planet. Inter.,* **25,** 297–356.

Ernst, R.E. & Buchan, K.L., 2003. Recognizing mantle plumes in the geological record, *Annu. Rev. Earth planet. Sci.,* **31,** 469–523.

Evans, D.A.D., 2010. Earth science: proposal with a ring of diamonds, *Nature,* **466,** 326–327.

Forte, A.M. & Mitrovica, J.X., 2001. High viscosity deep mantle flow and thermochemical structure inferred from seismic and geodynamic data, *Nature,* **410,** 1049–1056.

Grand, S.P., 2002. Mantel shear-wave tomography and the fate of subducted slabs, *Phil. Trans. R. Soc. Lond., A,* **360,** 2475–2491.

He, Y. & Wen, L., 2009. Structural features and shear-velocity structure of the 'Pacific Anomaly', *J. geophys. Res.,* **114,** B02309, doi:10.1029/2008JB005814.

Irifune, T., Shinmei, T., McCammon, C.A., Miyajima, N., Rubie, D.C. & Frost, D.J., 2010. Iron partitioning and density changes of pyrolite in Earth's lower mantle, *Science,* **327,** 193–195.

Kellogg, L.H., Hager, B.H. & van der Hilst, R.D., 1999. Compositional stratification in the deep mantle, *Science,* **283,** 1881–1884.

Kuo, B.-Y., Garnero, E.J. & Lay, T., 2000. Tomographic inversion of S-SKS times for shear velocity heterogeneity in D″: degree 12 and hybrid models, *J. geophys. Res.,* **105,** 28 139–28 157.

Masters, G., Laske, G., Bolton, H. & Dziewonski, A.M., 2000. The relative behavior of shear velocity, bulk sound speed, and compressional velocity in the mantle: implications for chemical and thermal structure, in *Earth's Deep Interior: Mineral Physics and Tomography from the Atomic to the Global Scale,* Geophysical Monograph, Vol. **117,** pp. 63–87, eds Karato, S., Forte, A.M., Liebermann, R.C., Masters, G. & Stixrude, L., AGU.

Mattern, E., Matas, J., Ricard, Y. & Bass, J., 2005. Lower mantle composition and temperature from mineral physics and thermochemical modeling, *Geophys. J. Int.,* **160,** 973–990.

McNamara, A.K. & Zhong, S., 2005. Thermochemical structures beneath Africa and the Pacific Ocean, *Nature,* **437,** 1136–1139.

Montelli, R., Nolet, G., Dahlen, F.A. & Masters, G., 2006. A catalogue of deep mantle plumes: new results from finite-frequency tomography, *Geochem. Geophys. Geosyst.,* **7**(11), Q11007, doi:10.1029/2006GC001248.

Mukhopadhyay, S., 2012. Early differentiation and volatile accretion recorded in deep-mantle neon and xenon, *Nature,* **486,** 101–106.

Ni, S., Tan, E., Gurnis, M. & Helmberger, D., 2002. Sharp sides to the African superplume, *Science,* **296,** 1850–1852.

Richards, M.A., Duncan, R.A. & Courtillot, V.E., 1989. Flood basalts and hotspot tracks: plume heads and tails, *Science,* **246,** 103–107.

Ritsema, J. & van Heijst, H.J., 2000. Seismic imaging of structural heterogeneity in Earth's mantle: evidence for large-scale mantle flow, *Sci. Prog.,* **83,** 243–259.

Schuberth, B.S.A., Zaroli, C. & Guust, N., 2012. Synthetic seismograms for a synthetic Earth: long-period P- and S-wave traveltime variations can be explained by temperature alone, *Geophys. J. Int.,* **188,** 1393–1412.

Sobolev, S.V., Sobolev, A.V., Kuzmin, D.V., Krivolutskaya, N.A., Petrunin, A.G., Arndt, N.T., Radko, V.A. & Vasiliev, Y.R., 2011. Linking mantle plumes, large igneous provinces and environmental catastrophes, *Nature,* **477,** 312–316.

Steinberger, B., 2000. Plumes in a convecting mantle: models and observations for individual hotsports, *J. geophys. Res.,* **105,** 11 127–11 152.

Steinberger, B. & Torsvik, T.H., 2012. A geodynamic model of plumes from the margins of large low shear velocity provinces, *Geochem. Geophys. Geosyst.,* **13,** Q01W09, doi:10.1029/2011GC003808.

Sun, D., Helmberger, D. & Gurnis, M., 2010. A narrow, mid-mantle plume below southern Africa, *Geophys. Res. Lett.,* **37,** L09302, doi:10.1029/2009GL042339.

Tan, E., Leng, W., Zhong, S. & Gurnis, M., 2011. On the location of plumes and lateral movement of thermochemical structures with high bulk modulus in the 3-D compressible mantle, *Geochem. Geophys. Geosyst.,* **12,** Q07005, doi:10.1029/2011GC003665.

Thorne, M.S., Garnero, E.J. & Grand, S.P., 2004. Geographic correlation between hot spots and deep mantle lateral shear-wave velocity gradients, *Phys. Earth planet. Inter.,* **146,** 47–63.

To, A., Romanowicz, B., Capdeville, Y. & Takeuchi, N., 2005. 3D effects of sharp boundaries at the borders of the African and Pacific superplumes: observation and modeling, *Earth planet. Sci. Lett.,* **233,** 137–153.

Torsvik, T.H., Smethurst, M.A., Burke, K. & Steinberger, B., 2006. Large igneous provinces generated from the margins of the large low-velocity provinces in the deep mantle, *Geophys. J. Int.,* **167,** 1447–1460.

Torsvik, T.H., Smethurst, M.A., Burke, K. & Steinberger, B., 2008a. Long term stability in deep mantle structure: evidence from the ∼300 Ma Skagerrak-centered large igneous province (the SCLIP), *Earth planet. Sci. Lett.,* **267,** 444–452.

Torsvik, T.H., Steinberger, B., Cocks, L.R.M. & Burke, K., 2008b. Longitude: linking Earth's ancient surface to its deep interior, *Earth planet. Sci. Lett.,* **276,** 273–282.

Torsvik, T.H., Burke, K., Steinberger, B., Webb, S.J. & Ashwal, L.D., 2010. Diamonds sampled by plumes from the core-mantle boundary, *Nature,* **466,** 352–355.

Zhang, N., Zhong, S.J., Leng, W. & Li, Z.X., 2010. A model for the evolution of the Earth's mantle structure since the Early Paleozoic, *J. geophys. Res.,* **115,** B06401, doi:10.1029/2009JB006896.

APPENDIX: CORRELATION BETWEEN THE VELOCITY AND GRADIENT FIELD AT LARGE IGNEOUS PROVINCE (LIP) LOCATIONS

We used a Monte Carlo approach to test whether one can distinguish between deep mantle plume sources that are located within regions of low seismic velocity or a zone defined by a range of velocity gradients. For this test, we adopt the S20RTS tomography model, which provides perturbations in shear wave velocity at a depth of 2800 km (Fig. 1a), and the smooth gradient of this field (Fig. 1b). We normalize these scalar fields so that if we repeatedly take the average of 24 randomly located values we obtain distributions with the same mean (of 0) and standard deviation (of 1) for both fields. Let V_i and G_i be the shear wave velocity and magnitude of the velocity gradient that the ith plume overlies. We define the test statistic, $\bar{E}$, as the mean of all $E_i = G_i + V_i$. We calculate the test statistic for the observed data, which results in $\overline{E_\mathrm{obs}} = -0.2$.

In the first Monte Carlo test, we compute $\bar{E}$ for 24 points that are distributed such that 21 are positioned within slow regions and three within fast regions as defined by the S20RTS model at 2800 km depth. This positioning matches the distribution of reconstructed LIP locations relative to the same tomographic model. We calculate a distribution for the statistic $\bar{E}$ from 10 000 repetitions (Supporting Information, Fig. S1a). Using this distribution, $\overline{E_\mathrm{obs}}$ is in the 91th percentile, that is 91 per cent of the Monte Carlo outcomes are smaller than the observed value. We conclude that if we prescribe the relative distribution of LIPs within slow and fast seismic velocity regions, we predict the observed range in velocity gradients that the LIPs overlie reasonably well (using a significance level of 95 per cent).

In the second Monte Carlo test, we repeatedly compute $\bar{E}$ for a set of 24 points that we locate within a specific range of velocity gradients. The observed distribution of velocity gradients sampled by LIPs is relatively uniform between approximately 0.04 and 0.11 per cent deg^{-1}, and so we assume a uniform distribution within this range for the 24 points in the Monte Carlo analysis. We calculate a distribution of $\bar{E}$ from 10 000 repetitions (Fig. S1b) and find that $\overline{E_\mathrm{obs}}$ is in the 0.6th percentile. Thus, if we prescribe a range of velocity gradients consistent with the observed distribution of LIPs, we poorly predict (at a 95 per cent confidence level) the velocity range sampled by the LIPs.

We conclude from these two tests that slow regions provide a better description of the preferred geographic location of plumes than a specific range of (high) velocity gradients.

SUPPORTING INFORMATION

Additional Supporting Information may be found in the online version of this article:

Figure S1. Results of Monte Carlo statistical testing (10 000 samples) based on the S20RTS seismic tomography model at 2800 km depth and the palaeomagnetic reference frame for LIP reconstruction (a) The distribution of $\bar{E}$ (mean sum of normalized velocities and normalized gradients in velocity) when 21 of 24 points are randomly positioned in regions of slower-than-average seismic shear wave velocity at 2800 km depth. The vertical red line denotes the value associated with the reconstructed LIP locations. (b) Same as frame (a), except that the 24 points are randomly located within the range of velocity gradients sampled by the reconstructed LIP locations. (http://gji.oxfordjournals.org/lookup/suppl/doi:10.1093/gji/ggt500/-/DC1).

Please note: Oxford University Press is not responsible for the content or functionality of any supporting materials supplied by the authors. Any queries (other than missing material) should be directed to the corresponding author for the article.